Research paper

Co-pyrolysis of sewage sludge and organic fractions of municipal solid waste: Synergistic effects on biochar properties and the environmental risk of heavy metals

Xingdong Wang [a,b], Victor Wei-Chung Chang [b], Zhiwei Li [a], Zhan Chen [a], Yin Wang [a,*]

[a] CAS Key Laboratory of Urban Pollutant Conversion, Institute of Urban Environment, Chinese Academy of Sciences, Xiamen 361021, China
[b] Department of Civil Engineering, 23 College Walk, Monash University, Victoria 3800, Australia

ABSTRACT

The introduction of heavy metal-free biomass into the sewage sludge (SS) pyrolysis can effectively improve the biochar properties and reduce the bioavailability and toxicity of heavy metals (HMs) in blended biochar. Herein, this study aimed to understand the biochar properties and associated environmental risks of HMs, by comparing the residual contents from the co-pyrolysis of SS with various organic fractions of municipal solid waste (OFMSW) at 550 °C and pyrolysis alone at different temperatures between 350 and 750 °C. The results indicated that, compared with SS pyrolysis alone, co-pyrolysis of SS with various OFMSW (except PVC) lead to lower biochar yields but with higher pH values (increased between 21.80% and 31.70%) and carbon contents (raised between 33.45% and 48.22%) in blended biochars, and the chemical speciation analysis suggested that co-pyrolysis further promoted the HMs transformation into more stable forms which significantly reduce the associated environmental risk of HMs in the blended biochars (the values of RI lower than 55.80). The addition of PVC, however, impeded biochar properties and compromised HMs immobilization during SS pyrolysis.

1. Introduction

In recent decades, the annual generation rate and amount of sewage sludge (SS) from wastewater treatment plants have skyrocketed due to the rapid urbanization and industrialization. The amount of SS in china had exceeded 30 million tons in 2015 and may hit 60–90 million tons by 2020 (Zheng et al., 2019). SS usually contains numerous toxic organic matter (e.g., hazardous organic micro-pollutants, polycyclic aromatic hydrocarbons-PAH, aromatic amines, and dyeing agents) (Zielinska and Oleszczuk, 2016) and high levels of heavy metals (HMs) (Chen et al., 2019; Sun et al., 2020), these poisonous substances (especially HMs) exhibit strong biological toxicity, which can easily cause serious unknown threat to humans, wildlife and environment (Xu et al., 2019; Li et al., 2014). Meanwhile, SS has been considered as bio-resource and alternative mines owing to its high contents of bio-degradable organic matters and nutrients, which has aroused significant interests in the research areas (Chhabra et al., 2019; Chen et al., 2020; Marin-Batista et al., 2020). Therefore, how to treat SS appropriately by using an economically-feasible and environmentally-friendly technology has become a very important global emergency task.

Among the SS disposing technologies, the conventional approaches, such as ocean dumping, sanitary landfill and land application, have been restricted owing to the poisonous leachate and limited land resources (Li et al., 2018). Thermochemical treatment has attracted increasing attention over the past decade, especially the pyrolysis technology (Zheng et al., 2019). Pyrolysis, as one of the most promising thermochemical process for safe disposal of SS, possesses several advantages over sanitary landfill and incineration because of its energy recovery, nutrient recycling, HMs immobilization, and high-quality biochar production (Liu et al., 2017; Ahmed and Hameed, 2020; Chanaka Udayanga et al., 2019; Fan et al., 2020). The residual product of SS pyrolysis (biochar), a carbonaceous material intentionally, typically have a satisfactory surface adsorption site, large surface area with high porosity, high pH value, and great cation exchange capacity (El-Naggar et al., 2019). Owing to its characteristics, biochar is widely used as the soil remediation reagent to improve fertility, carbon sequestration, neutralize acidity, and HMs immobilization in polluted soil (Hagemann et al., 2017), as well as the cost-effective adsorbent to remove organic and HMs contaminants from aqueous phase (Ho et al., 2017; Yin et al., 2020). Considering the HMs severe negative impacts on living

organisms, the environmental risk associated with HMs accumulated in biochar have drawn much attention (Palansooriya et al., 2020). The most common HMs in SS are Zn, Cu, Cr, Pb, Ni, and Cd because they tend to have higher concentration and potential environmental risk. Many researchers had contributed their efforts in advancing the knowledge on the transformation, distribution and speciation evolution of HMs in SS during pyrolysis process (Chanaka Udayanga et al., 2019, 2018; Dou et al., 2017). During SS pyrolysis at the predominantly moderate temperatures, the majority of HMs were redistributed into the solid product (biochar) due to their higher thermal stability than organic substances (Chanaka Udayanga et al., 2019; Wang et al., 2019). While the chemical speciation of HMs can be transferred from the bioavailability and eco-toxicity fractions to more stable forms, this suggests pyrolysis process can immobilize the HMs in SS (Sun et al., 2018; Devi and Saroha, 2014; Wang et al., 2016). However, biochar produced from SS alone is not a suitable material as soil remediation reagent or environmental adsorbent because of its high ash content, low C content, small specific surface area, and high concentrations of HMs (Ahmed and Hameed, 2020; Wang et al., 2019). These drawbacks serious limit its large-scale agricultural and environmental applications in the future.

Co-pyrolysis can efficiently enhance the properties of biochar by processing the two or more feedstocks under the same operating condition. In this context, the additions of HM-free biomass wastes for co-pyrolysis with SS can contribute to increasing the C content, reducing the ash content, building well-developed pore structure, and diluting HMs concentrations of blended biochar (Tian et al., 2019; Wang et al., 2019; Chen et al., 2019; Dong et al., 2019). For instance, Jin et al., (2017) indicated that the addition of bamboo sawdust into SS promoted more unstable toxic HMs in SS transformed into more stable forms compared with single pyrolysis. In contrast, Huang et al. (2017) observed that co-pyrolysis of SS with rice straw/sawdust significantly reduced the total concentrations of HMs in biochar, while not observed the reduction of the HMs leaching toxicity in biochar. Suggesting that co-pyrolysis has inconsistent effects on the properties and HMs behaviors of the blended biochar, depending largely on feedstock type and pyrolysis operating condition. However, a systematic comparative research on the effects of biomass waste additions on the biochar properties and environmental risk associated with HMs have not been completed so far.

The organic fractions of municipal solid waste (OFMSW) are promising biomass wastes due to their large amount of production and urgency of safe disposal, which taken up approximately 62% of municipal solid waste in developing countries including China. The compositions of OFMSW depend on the social-geographical status and local living styles of the local human settlements, and on whether the collected OFMSW undergoes classification and resource recovery as part of its final disposal. Moreover, the specific proportion of compositions in OFMSW varies in different places, mainly determined by the local living styles and social-geographical status. In China, the OFMSW consists of agricultural waste, garden waste, food waste, plastics, paper, and fabric, while the paper and fabric wastes are often considered as the recyclable waste as they can create higher value-added benefits (Tokmurzin et al., 2020; Soomro et al., 2020). The OFMSW is rich in C content with skeletal molecules, and might be a suitable biomass wastes additive to enhance the biochar properties and promote the immobilization of HMs during SS pyrolysis. According to our knowledge, much more attention has been focused on products characteristics and kinetic analysis from co-pyrolysis of SS and various OFMSW so far (Chhabra et al., 2019; Yang et al., 2018), there still present few studies about the co-pyrolysis of SS and various OFMSW, and their synergistic effects on lowing the total concentrations and bioavailability of HMs and reducing potential environmental risks associated with HMs of biochar. An in-depth investigating of biochar properties and HMs behaviors from co-pyrolysis of SS and various OFMSW should be implemented to fill this gap.

To better represent the common OFMSW, we selected the bamboo sawdust (BS), wood sawdust (WS), rice husk (RH), exhausted tea (ET),

kitchen waste (KW), and polyvinyl chloride (PVC) as our targeted additives. Our previous practical pilot-scale test found that the addition of approximately 20% biomass for co-pyrolysis can generate sufficient bio-oil and syngas to satisfy the energy consumption which is required for co-pyrolysis at 550 °C (Li et al., 2018). Moreover, the pyrolysis process can immobilize HMs in biochar matrix only when the temperature is high enough (Chanaka Udayanga et al., 2019; Devi and Saroha, 2014), while the Cd exists mainly as a carbonate in SS and can be volatilized and transferred into liquid phase (bio-oil) when the temperature increased up to 600 °C (Wang et al., 2016). The Cd-contaminated bio-fuel could easily cause a dispersal of secondary contamination to impose adverse impacts on nearly all biological processes. To resolve these conflicting, we set the co-pyrolysis temperature of SS and various OFMSW at 550 °C would like to achieve the objective of the efficient retention and immobilization of all HMs in blended biochars, the temperature of SS pyrolysis alone was set at 350 °C, 550 °C, 750 °C to compare biochar properties and associated environmental risks of HMs with blended biochars from the co-pyrolysis of SS with various OFMSW. The objectives of this study includes: 1) to validate the synergistic effects of various OFMSW additions on biochar properties, 2) to reveal the chemical speciation evolution and immobilization of HMs in the biochars before and after additions of various OFMSW, and 3) to assess the phytotoxicity and potential environmental risk of HMs in the biochars.

2. Materials and methods

2.1. Materials and biochar preparation

SS was obtained from a municipal wastewater treatment plant in Xiamen City, China; BS, and WS, RH were collected from the farms in near-by suburbs; ET was collected from a local teahouse; KW was collected immediately after the greases removal at the Xiamen Eastern Solid Waste Management Center; and PVC powders with the particle size below 0.3 mm were sourced from an chemical store, China. All feedstocks (except PVC) went through a standardized pretreatment includes dried at 105 °C in an oven for 24 h, grounded into fine particles (100 mesh), and then stored in a desiccator at room temperature to maintain their low moisture before pyrolysis.

A single-step pyrolysis process was used to convert SS to biochar (as a comparison) at 350, 550 or 750 °C according to the procedure reported previously (Han et al., 2014), and co-pyrolysis of SS and various OFMSW were conducted at 550 °C following a similar protocol. Pyrolysis tests were carried out in a homemade pyrolysis experimental apparatus included a pyrolysis atmosphere supply system, a fixed bed quartz reactor with a surrounding electrically heated furnace, and a bio-oil and syngas absorption derive system (Fig. S1). In each pyrolysis test, 20.0 g of oven-dried SS or thoroughly mixed feedstocks (SS/various OFMSW, 4:1, w/w) were first loaded into a fixed bed quartz reactor with a nitrogen gas of 99.99% purity to wipe out the oxygen gas for 0.5 h before pyrolysis, and then the pyrolysis temperature increased to the target temperature at a rate of 10 °C min^{-1} with a pure nitrogen flowrate at 100 ml min^{-1}. The final pyrolysis residue (biochar) was natural cooled down in the quartz reactor after maintained for 1 h at target temperatures. The biochar derived from SS pyrolysis at X (°C) temperature was denoted as SSB-X, and the blended biochars from co-pyrolysis with BS, WS, RH, ET, KW, and PVC at 550 °C were labeled as SSB-BS, SSB-WS, SSB-RH, SSB-ET, SSB-KW, and SSB-PVC, respectively. Each pyrolysis condition was repeated three times and the biochars were homogeneously mixed and stored in a sealed plastic bag in desiccators before analysis.

2.2. Biochars properties analysis

The biochar yields represent the weight ratios of biochar to the original feedstock. The ash contents of feedstocks and biochars were calculated using the standard GB/T 12496.3–1999 (MEP, 1999). The pH

of the samples (sample: deionized water = 1:20, w/v) were measured by a digital pH meter (UB-7, Denver, USA). The element compositions (C, H, N, and S) of feedstocks and biochars were analyzed with an automatic elemental analyzer (Vario EL III, Hanau, Germany). The specific surface area (SSA) of SS and biochars were detected by N_2 adsorption-desorption isotherms at 77 K with an automated surface area and pore size analyzer (ASAP 2020, Micromeritics, USA). To identify the surface functional groups of SS and biochars, the oven-dried samples were mixed with KBr at a ratio of 1:100 and then pressed into a pellet in a Fourier transform infrared (FTIR) spectrometry (NicoletiS10, Thermo-Fisher, USA). The spectra were recorded in the range of 400–4000 cm^{-1} at a resolution of 4 cm^{-1}.

2.3. Analysis of HMs

2.3.1. Chemical speciation of HMs

The chemical speciation of HMs (Zn, Cu, Cr, Pb, Ni, and Cd) in SS and biochars were analyzed by a modified three-step BCR sequential extraction procedure (Zhang et al., 2020), which classified the HMs into four fractions: exchangeable/acid-soluble fraction (F1); reducible fraction (F2, associated with Fe and Mn oxides); oxidizable fraction (F3, bound to organic matter); and a residual fraction (F4) (Li et al., 2018). The suspensions for the F1, F2, and F3 collected from each step were digested with a mixed acid (HNO_3/H_2O_2 = 1: 1, v/v.) to remove dissolved organics. The feedstocks, biochars, and the BCR extracted solid residues were digested with a mixed acid (HNO_3: $HClO_4$: HF = 5: 5: 2, v/v) by using the microwave digestion. All the digested solutions were filtered through a 0.22 μm nylon filter, and then diluted to a constant volume of 50 ml with HNO_3 (0.5%) before analysis. The concentrations of Zn, Cu, Cr, Pb, Ni, and Cd were determined by ICP-MS (7500CX, Agilent Technologies, USA).

2.3.2. Leaching characteristics of HMs

To evaluate the HM leachability under different environmental conditions, we selected two common protocols. The standard toxicity characteristic leaching procedure (TCLP) simulates landfill condition by using the glacial acetic acid solution (pH: 2.88) to illustrate the immobilization capacity of HMs (Nair et al., 2008). Another protocol uses 0.005 M diethylenetriamine pentaacetic acid solution (DTPA), 0.1 M triethanolamine (TEA), and 0.01 M $CaCl_2$ at pH= 7.3 to assess the plant-available of HMs in SS and biochars (He et al., 2019). One gram of over-dried sample was extracted by 20 ml leaching solutions in a shaking incubator at 200 rpm for 18 h. The supernatant was separated by centrifugation and subsequently digested with a mixed acid (HNO_3/H_2O_2 = 1:1, v/v.) to remove dissolved organics for HMs analysis.

2.4. Phytotoxicity assessment and environmental risk evaluation

2.4.1. Phytotoxicity assessment

Germination index (GI) is a widely used indicator to assess the phytotoxic impacts of HMs to the plant growth (Shen et al., 2020). One gram of the SS or biochar was extracted by 10 ml of deionized water at 200 rpm and 25 °C for 2 h. 5 ml of the filtrate was added into the pre-sterilized petri dish with 10 cucumber seeds uniformly scattered on the wetted filter paper. The petri dishes were incubated in a dark incubator at 25 °C for 72 h. Germination index (GI) was calculated using the following equation:

$$GI = (N_i \times L_i)/(N_c \times L_c) \tag{1}$$

where N_i is the number of germinated seeds in treatment, N_c is the number of germinated seeds in the control using deionized water, L_i is the mean root length in treatment and L_c is the mean root length in control.

2.4.2. Environmental risk evaluation

Risk assessment code (RAC) and potential ecological risk index (RI)

have been widely used to evaluate the potential environmental risk (Shen et al., 2020). RAC represents the availability of single HMs in the environment using the percentage of HMs in the F1 fraction, which classified the risk into five types: no risk (NR), RAC ‹ 1%; low risk (LR), 1%≤ RAC ‹10%; medium risk (MR), 10%≤ RAC ‹ 30%; high risk (HR), 30%≤ RAC ‹50%; very high risk (VHR), RAC ≥ 50%. And RI indicates the environmental risks associated with multi-HMs and calculated using the following equations:

$$C_f = C_m/C_n \tag{2}$$

$$E_r = T_r \times C_f \tag{3}$$

$$RI = \sum E_r \tag{4}$$

where, C_f is the individual HMs contamination factor; C_m and C_n are the content of each individual HMs distributed in potential mobile fractions (F1 + F2 + F3) and a stable fraction (F4), respectively; E_r is the potential ecological risk index for individual HMs; T_r is the toxic factor of each individual HMs, and the T_r values for each individual HMs are in the order of Zn (1), Cr (2), Cu (5), Ni (6), Pb (5), and Cd = 30 (Huang and Yuan, 2016); RI is the potential ecological risk index for the overall contamination.

3. Results and discussions

To achieve the objectives set out previously, the discussion section firstly covered the physicochemical properties analysis and the FTIR spectra to validate the synergistic effects of OFMSW additions on biochar properties. The chemical speciation evolution and HM immobilization before and after the OFMSW additions were also illustrated using the results from total concentrations, chemical speciation, and leaching characterization of HMs analysis. The final section focused on phytotoxicity and environmental risk of SS and the derived biochars.

3.1. Properties of the SS and biochars

3.1.1. Physicochemical properties

Table 1 showed the physicochemical properties of the SS and biochars derived from pyrolysis of SS alone and co-pyrolysis of SS with various OFMSW. By comparing the biochars under different temperatures (SSB 350–750), the yields were reversely associated with the rise of temperature. In addition, the yield drop between 350 and 550 °C (82. 07–62.71%) was higher than that between 550 and 750 °C (62.71–60.31%). Both suggested that the decreases are mainly associated with the decomposition of organic matter in SS during the pyrolysis process, and most of organic substances were decomposed between 350 and 550 °C (Agrafioti et al., 2013; Yuan et al., 2015). The ash contents for biochar also increased with higher temperature, implying most of the inorganic constituents in SS were retained in biochars after pyrolysis.

The additions of OFMSW seemed to decrease both biochar yields and ash contents while significantly increased the biochar yield after ash deduction and C contents, as comparing to SSB-550 (Table 1). As these OFMSW have relatively lower ash contents between 0.55% and 12.21% with much higher C contents between 38.67% and 49.12% than SS (Table S1), the mixed ratio at 4:1 (SS: OFMSW. w/w) leads to higher organic fractions in the SS and OFMSW mixtures. The blended biochar yields showed 4.83–9.98% decrease comparing to SSB-550, while the ash contents dropped between 6.65% and 12.25%. This implies that the additions of OFMSW contributed to the reduction of the inorganic salt fraction in the biochars.

Increasing temperature in pyrolysis also led to the reduction of C, H, N, and O as part of the organic substance transformation. It was worth noting that element S showed a different trend with the rise of temperature because it might remain in biochar as stable sulfur-containing inorganic substances (Liu et al., 2020). The ratio of molar H/C can

Table 1
Physicochemical properties of the SS and biochars on dry basis[a].

Samples	Y_A (%)	Y_D (%)	Ash (%)	pH	C (%)	H (%)	N (%)	S (%)	O[b] (%)	H/C	SSA (m² g⁻¹)
SS	/	/	49.01 ± 0.89	6.85 ± 0.05	26.24 ± 0.85	6.02 ± 0.30	3.04 ± 0.01	2.32 ± 0.19	13.37	2.75	0.92
SSB-350	82.07 ± 0.52	68.28	57.58 ± 0.99	6.97 ± 0.08	24.07 ± 0.33	5.13 ± 0.21	2.69 ± 0.02	1.95 ± 0.01	8.58	2.56	0.56
SSB-550	62.71 ± 1.12	26.58	78.39 ± 0.59	7.57 ± 0.11	14.35 ± 0.03	0.85 ± 0.02	2.02 ± 0.03	2.01 ± 0.02	2.40	0.71	31.30
SSB-750	60.31 ± 0.71	19.76	83.29 ± 1.06	10.81 ± 0.06	13.63 ± 0.04	0.82 ± 0.07	1.55 ± 0.02	2.38 ± 0.03	1.29	0.75	44.82
SSB-BS	59.68 ± 0.85	35.22	69.91 ± 0.56	9.97 ± 0.08	21.06 ± 0.39	0.85 ± 0.02	1.89 ± 0.02	1.94 ± 0.01	4.34	0.49	20.36
SSB-WS	56.51 ± 0.59	34.37	68.99 ± 0.14	9.22 ± 0.05	21.27 ± 0.62	0.85 ± 0.01	1.88 ± 0.02	1.88 ± 0.01	5.12	0.48	14.71
SSB-RH	58.38 ± 0.77	33.51	70.73 ± 0.33	9.29 ± 0.03	20.25 ± 0.42	0.89 ± 0.01	1.96 ± 0.01	1.99 ± 0.01	4.18	0.53	16.07
SSB-ET	56.45 ± 1.07	34.55	68.79 ± 0.52	9.60 ± 0.12	19.68 ± 0.30	0.86 ± 0.01	2.28 ± 0.03	2.11 ± 0.02	6.28	0.53	22.16
SSB-KW	57.37 ± 1.33	30.18	73.18 ± 0.31	9.68 ± 0.13	19.15 ± 1.61	0.91 ± 0.02	2.61 ± 0.04	2.12 ± 0.03	2.03	0.57	12.11
SSB-PVC	57.20 ± 0.22	33.56	70.08 ± 0.29	3.06 ± 0.21	19.99 ± 1.17	0.96 ± 0.04	1.82 ± 0.01	1.33 ± 0.04	5.82	0.57	2.20

SS, sewage sludge; SSB-X, biochar derived from SS single pyrolysis at X (°C) temperature; SSB-BS, SSB-WS, SSB-RH, SSB-ET, SSB-KW, and SSB-PVC were blended biochars from co-pyrolysis SS with bamboo sawdust (BS), wood sawdust (WS), rice husk (RH), exhausted tea (ET), kitchen waste (KW), and polyvinyl chloride (PVC) at 550 °C, respectively; Y_A: the biochar yield before ash deduction; Y_D: the biochar yield after ash deduction; SSA, specific surface area.
[a] Values are the mean ± SD (standard deviation) of three replicated tests.
[b] By difference, O = 100–(C + H + N + S+ Ash).

provide more insights regarding the degree of organic aromaticity of biochar, a molar H/C ratio ≤ 0.3 generally suggests a high fraction of condensed aromatic ring structures whereas ≥ 0.7 indicates a low fraction (Jin et al., 2017). The molar H/C ratio decreased during the pyrolysis and was sensitive to the temperatures. Comparing SSB350 (H/C = 2.56) with SSB550 (H/C = 0.71) and SSB750 (H/C = 0.75), the notable higher reduction from 350 to 550 °C means that the decarboxylation and demethylation reactions mainly occurred before 550 °C during pyrolysis. This finding is consistent with the results of the yield drop.

It was worth noting that, after the additions of OFMSW under the same temperature at 550 °C, the C contents of the SSB-BS, SSB-WS, SSB-RH, SSB-ET, SSB-KW, and SSB-PVC raised by 46.76%, 48.22%, 41.11%, 37.14%, 33.45%, and 39.30%, respectively, compared with that in the SSB-550. This C sequestration is beneficial as it can enhance the agronomic performance of biochar as a soil amendment to address climate change and soil degradation (Hagemann et al., 2017; Nottingham et al., 2020). All OFMSW mixtures produced the biochars with lower H/C ratios (H/C ≤ 0.57) implying the increase in aromatic structure, making the biochars less susceptible to oxidation in various environmental applications such as soil remediation (Du et al., 2019).

The pH values of biochar were higher than SS and exhibited a positive correlation with the temperature, mainly owing to the transformation of alkali salts and the decomposition of acidic surface functional groups as reported in previous studies (Jin et al., 2016; Wang et al., 2019). It was worth noting that the additions of various OFMSW presented inconsistent changes in pH values. The pH values of the SSB-BS, SSB-WS, SSB-RH, SSB-ET, and SSB-KW were 9.97, 9.22, 9.29, 9.60, and 9.68, respectively. Comparing with SSB-550 (7.57), the additions of BS, WS, RH, ET, and KW resulted in a remarkable increase of pH between 21.80% and 31.70%, possibly because the additions promoted the transformation of metallic compounds to the alkali salts and the decomposition of acidic surface functional groups. Especially for the SSB-BS with highest pH, mainly due to the BS addition enhanced aromaticity of SSB-BS (Jin et al., 2017). The addition of PVC, however, showed the lowest pH value (3.06), implying a significant portion of HCl molecules during PVC pyrolysis remained in biochar (Cao et al., 2019). The SSA of blended biochars were consistently lower that of SSB-550, mostly likely due to the amounts of tars produced from the thermal degradation of hemicellulose and cellulose in the added OFMSW because those tars tend to adhere to the surface and block the porous structure of biochars (Jin et al., 2017; Huang et al., 2017). Among various OFMSW, SS-PVC produced the most significant reduction in SSA (2.20 m² g⁻¹) comparing to SSB-550 (31.30 m² g⁻¹). The HCl released from PVC pyrolysis promoted the transformation of light tar to heavy components (Tang et al., 2018) which further adhere and block the porous structures. A similar result was reported in the co-pyrolysis of pine wood (PW) and PVC where PW-PVC interaction significantly

decreased the biochar SSA (Lu et al., 2018).

3.1.2. FTIR spectra analysis

FTIR spectra analysis provides insights regarding the changes of the functional groups in SS and biochars. Fig. 1A showed the intensity of the peak around 3400 cm⁻¹ (-OH stretching vibration) decreased significantly from SS to biochars, suggesting that the large number of hydroxyl groups associated to water, carboxylic acids, and alcohols were decomposed as the temperature increased. The additions of OFMSW slightly enhanced the intensity of -OH stretching vibration (3400 cm⁻¹) in blended biochars comparing to SSB-550. This is favorable as it enhances the biochar quality in terms of adsorption capacity as the soil amendment or adsorbent. The peaks around 2800–3000 cm⁻¹ (asymmetrical and symmetrical -CH$_n$ stretching) disappeared when the temperature goes higher than 550 °C, suggesting that organic fatting hydrocarbons in SS were completely decomposed (Jin et al., 2016). This is further supported by some other indicators such as the peak around 1438 cm⁻¹ (CH$_3$ and CH$_2$ groups which corresponds to aliphatic chains) disappeared as the pyrolysis temperature increased above 550 °C. In addition to the chain-structure hydrocarbons, the intensity of the peak at 1654 cm⁻¹ (C=C, C=O, and –CONH- stretching vibration that associates to stretching amide bonds and aromatic rings) (Jin et al., 2016) decreased only slightly with the rising temperature, indicating that the aromatic structure in the biochar does not significantly affected by the temperature. The retention of this structure further implies the formation of condensed aromatic structure in biochar. Similar trends were observed on peaks around 1032 cm⁻¹ (C-O-C aliphatic/stretching) and below 600 cm⁻¹ (generally described as metal-halogen stretching vibrations) (Jin et al., 2016), indicating the rising temperature does not affect these functional groups significantly. The above results showed that the intensity and category of the chemical functional groups in biochar dramatically affected by pyrolysis temperature, and the additions of OFMSW can be beneficial to the retention of -OH stretching vibration in the blended biochars.

3.2. Analysis of HMs

3.2.1. Total concentrations of HMs

Regarding the total concentrations of HMs (Zn, Cu, Cr, Pb, Ni, and Cd) in SS and biochars (Table 2), the six HMs followed the sequence: Zn > Cu > Cr > Pb > Ni > Cd. The content of Zn (1729.80 mg kg⁻¹) among HMs in SS was the highest, likely ascribing to the widely used of galvanized pipes in wastewater pipelines of China (Jin et al., 2017). After pyrolysis of SS, the total Zn, Cu, Cr, Pb, and Ni concentrations in biochar gradually increased with rising temperature, Fig. 2 also showed that the residual rates of Zn, Cu, Cr, Pb, and Ni in biochars were over 93.59%, indicating that most of these HMs were mainly redistributed in biochars owing to their relatively lower vapor pressures and higher
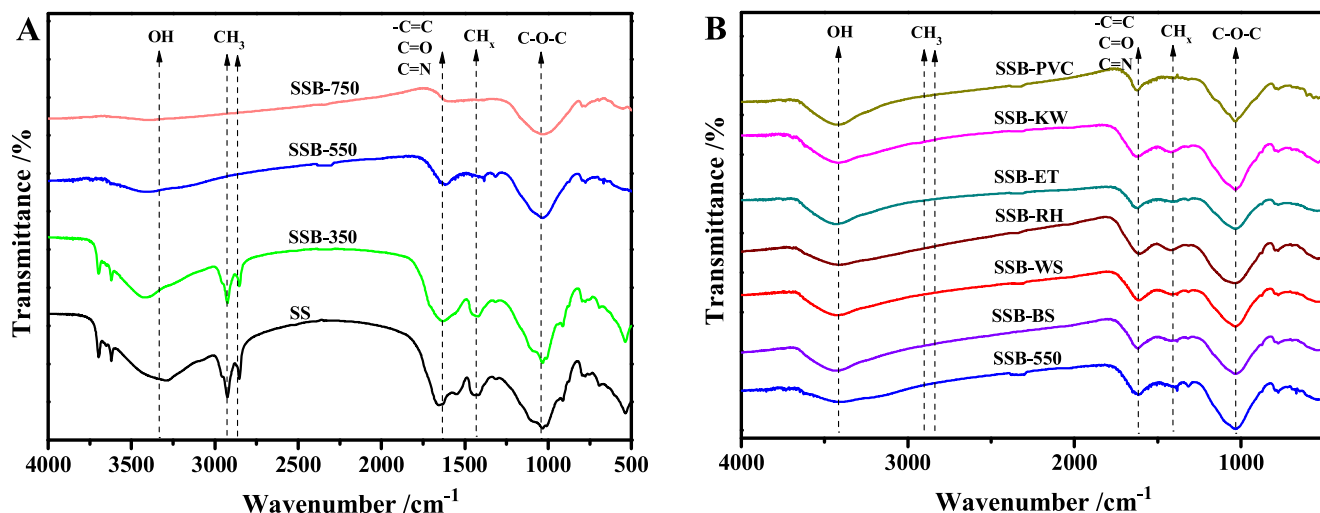
Fig. 1. FTIR spectra of (A) SS and biochars derived from pyrolysis of SS alone under different temperatures, and (B) biochars from co-pyrolysis of SS and various OFMSW. SS, sewage sludge; SSB-X, biochar derived from SS single pyrolysis at X (°C) temperature; SSB-BS, SSB-WS, SSB-RH, SSB-ET, SSB-KW, and SSB-PVC were blended biochars from co-pyrolysis SS with bamboo sawdust (BS), wood sawdust (WS), rice husk (RH), exhausted tea (ET), kitchen waste (KW), and polyvinyl chloride (PVC) at 550 °C, respectively.

Table 2
Total concentrations of HMs in SS and biochars.

Samples	Heavy metals (mg kg^{-1})[a]					
	Zn	Cu	Cr	Pb	Ni	Cd
SS	1729.80 ± 11.23	111.83 ± 2.65	94.25 ± 4.33	50.08 ± 1.94	30.92 ± 1.42	1.22 ± 0.05
SSB-350	2059.72 ± 18.75	134.67 ± 4.74	110.59 ± 5.79	62.39 ± 2.07	37.38 ± 1.54	1.53 ± 0.15
SSB-550	2602.93 ± 17.58	169.93 ± 3.66	142.90 ± 3.89	78.54 ± 1.59	49.31 ± 2.05	2.01 ± 0.09
SSB-750	2763.47 ± 13.94	178.91 ± 2.55	150.93 ± 7.12	81.65 ± 0.98	50.18 ± 0.45	0.45 ± 0.01
SSB-BS	2364.90 ± 22.12	150.90 ± 5.28	124.37 ± 6.02	67.61 ± 1.03	38.98 ± 1.22	1.54 ± 0.11
SSB-WS	2308.24 ± 13.56	149.38 ± 5.91	130.95 ± 2.81	70.82 ± 0.85	42.91 ± 1.15	1.71 ± 0.14
SSB-RH	2354.77 ± 20.58	155.06 ± 2.77	201.16 ± 4.74	68.82 ± 0.37	74.27 ± 0.44	1.72 ± 0.06
SSB-ET	2351.62 ± 19.83	153.41 ± 3.18	131.51 ± 4.01	71.60 ± 0.46	41.50 ± 0.59	1.68 ± 0.04
SSB-KW	2308.05 ± 15.73	153.07 ± 4.43	141.35 ± 1.99	70.67 ± 1.20	42.76 ± 0.82	1.79 ± 0.05
SSB-PVC	2264.28 ± 10.36	153.93 ± 3.99	132.45 ± 3.07	69.38 ± 1.14	40.65 ± 1.95	1.64 ± 0.11

SS, sewage sludge; SSB-X, biochar derived from SS single pyrolysis at X (°C) temperature; SSB-BS, SSB-WS, SSB-RH, SSB-ET, SSB-KW, and SSB-PVC were blended biochars from co-pyrolysis SS with bamboo sawdust (BS), wood sawdust (WS), rice husk (RH), exhausted tea (ET), kitchen waste (KW), and polyvinyl chloride (PVC) at 550 °C, respectively.

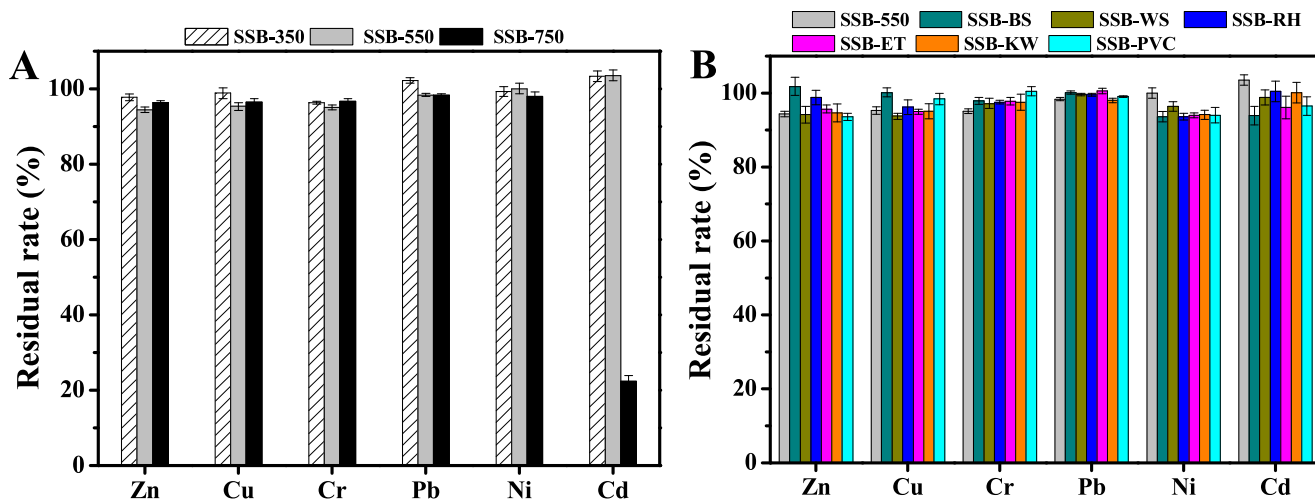[a] Values are the mean ± SD (standard deviation) of three replicated tests.

Fig. 2. The residual rate of HMs in biochars derived from (A) pyrolysis of SS alone under different temperatures and (B) co-pyrolysis of SS and various OFMSW. SSB-X, biochar derived from SS single pyrolysis at X (°C) temperature; SSB-BS, SSB-WS, SSB-RH, SSB-ET, SSB-KW, and SSB-PVC were blended biochars from co-pyrolysis SS with bamboo sawdust (BS), wood sawdust (WS), rice husk (RH), exhausted tea (ET), kitchen waste (KW), and polyvinyl chloride (PVC) at 550 °C, respectively.

boiling temperatures. While the contents of Cd in biochars gradually increased as the temperature increasing before 550 °C, then decreased suddenly when the temperature increased to 750 °C. For instance, the residual rate of Cd in SSB-750 was only 22.34% (Fig. 2). The reason for less retention of Cd in SSB-750 ascribing to its strong volatility (Xu et al., 2019). A similar observation was made by other researchers (W et al., 2019; Devi and Saroha, 2014). Cd in SS existed mainly as a carbonate which can be easily volatilized into the gas stream when the temperature increased up to 600 °C (Kistler et al., 1987).

As most of the OFMSWs have low HMs contents (Table S2), the additions of OFMSW generally led to a reduction of HMs in blended biochars due to the "dilution effect". The only exception is the SSB-RH (rice husk) where the high Cr and Ni in the original RH contributed to the corresponded concentration in the biochars. Overall, the additions of OFMSW with a pyrolysis temperature not exceeding 550 °C is a potential approach to decrease the total HM levels of blended biochars and further enhance the suitability for soil remediation application.
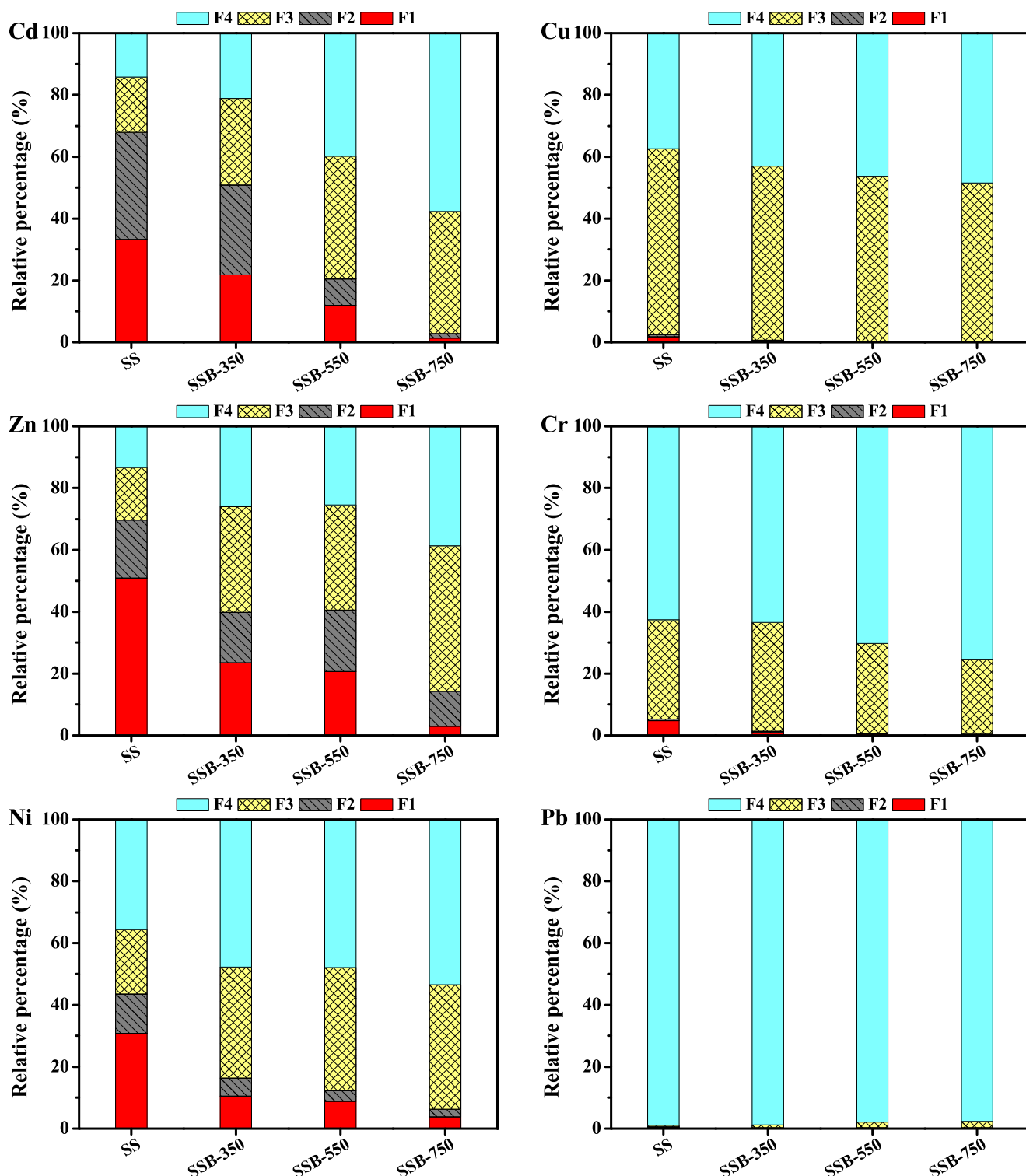

Fig. 3. Fraction distribution of HMs in SS and biochars. SS, sewage sludge; SSB-X, biochar derived from SS single pyrolysis at X (°C) temperature.

3.2.2. Chemical speciation of HMs

The bioavailability and eco-toxicity of HMs in SS and biochars not only lie on the total concentrations, but also depend on the chemical speciation (Huang and Yuan, 2016; Yuan et al., 2011). According to the results from a modified three-step BCR described in the method section, the bioavailability of HMs decrease in the following sequence: F1 > F2 > F3 > F4 (Li et al., 2018). The HMs fractions can be classified into three categories according to their mobility and degradation resistance: 1) F1 + F2 are associated with high bioavailability and direct eco-toxicity, 2) F3 indicated a potential bioavailability and eco-toxicity as it is relatively degradable in the environment, 3) F4 shows low bioavailability and toxicity (Devi and Saroha, 2014). The HM recovery during this sequential extraction serves as a quality control indicator. The results showed a good agreement between the sum of each fraction and the total HMs concentration with a satisfactory recovery between 95.00% and 105.86% (Table S3).
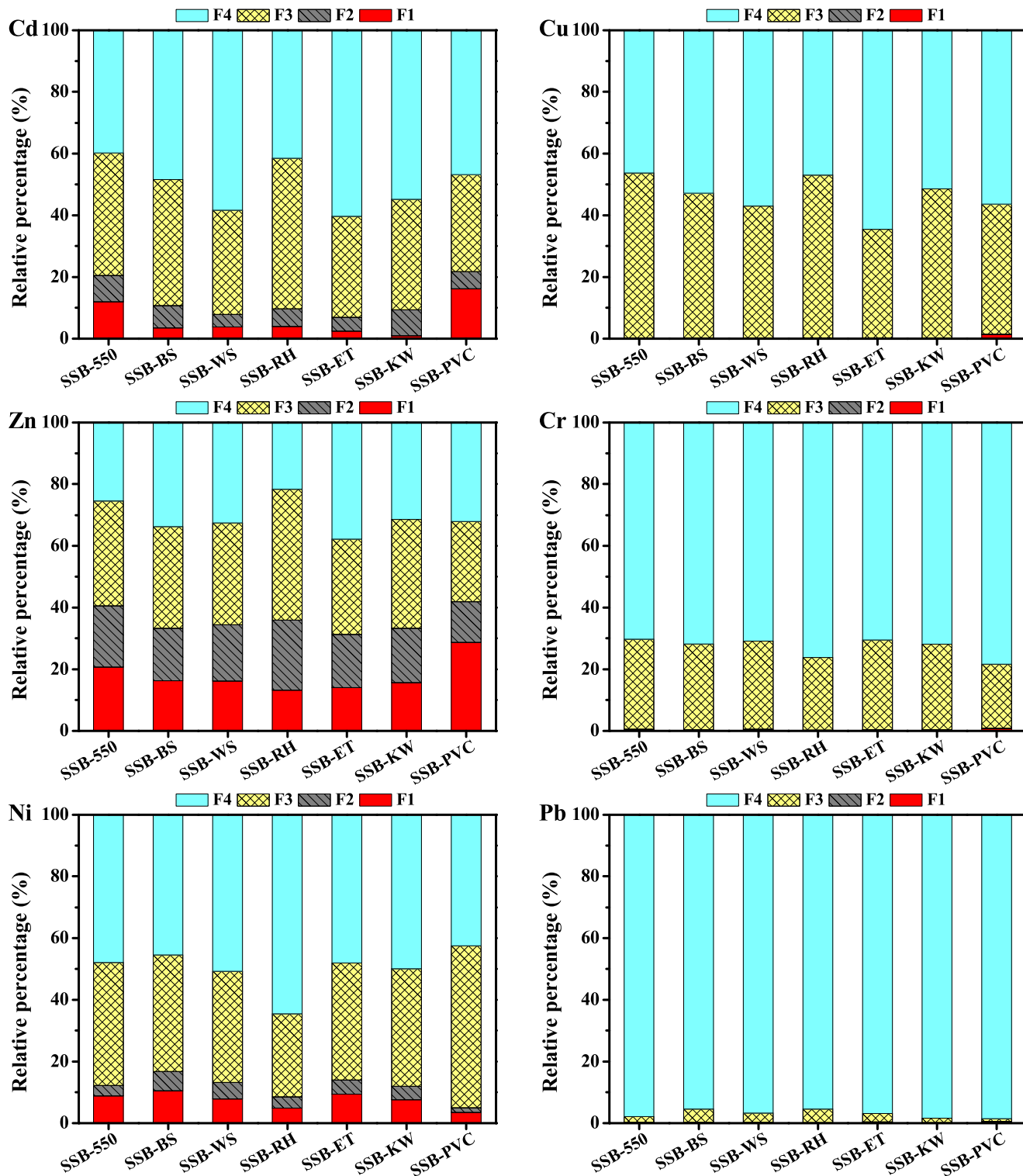

Fig. 4. Fraction distribution of HMs in blended biochars. SSB-BS, SSB-WS, SSB-RH, SSB-ET, SSB-KW, and SSB-PVC were blended biochars from co-pyrolysis SS with bamboo sawdust (BS), wood sawdust (WS), rice husk (RH), exhausted tea (ET), kitchen waste (KW), and polyvinyl chloride (PVC) at 550 °C, respectively.

Fig. 3 revealed significant differences in HMs' distribution patterns in the raw SS. Among the six HMs investigate, Zn, Cd and Ni had much higher F1 and F2 fractions comparing to the others. More than 67% of Zn and Cd in SS were in F1 + F2 and Ni also had a high ratio at 43%, which suggested a higher potential environmental risk from Zn, Ni, and Cd if the SS is directly applied to the soil. Over 94% of Cu and Cr in SS presented in F3 + F4 fractions while almost all of Pb remained in F4. This implies that the Cu and Cr mainly existed in the organic and residual phases (Wang et al., 2019; Shi et al., 2013) and Pb was associated with the primary minerals in SS (Wong et al., 2001). This observation was consistent with the findings in previous studies (Devi and Saroha, 2014; Wang et al., 2016; Jin et al., 2016).

When converting SS into biochars via single pyrolysis, the bioavailability portion (F1 + F2) decreased when temperature rises (Fig. 3). For example, the bioavailability of Cd in the biochar reduced from 50.83% in SSB-350 to 20.41% in SSB-550 and then 2.74% in SSB-750. While Cd in SS mainly associate with carbonate and phosphate, a large proportion, such as $Cd(H_2PO_4)_2$, can be dissolved in acetic acid solution (F1 fraction) (Zhang et al., 2019). Pyrolysis of SS at a lower temperature can improve the Cd stability by forming Cd oxides or carbon matrix as organometallic compounds. Further increase the temperature above 600 °C can decompose phosphate into Cd oxide and then volatilized into the gas stream, which lead to a small retention of organometallic compounds in biochar (Kistler et al., 1987). As to Zn and Ni, pyrolysis under low temperatures did reduce the bioavailability but temperature increase from 350 to 550 °C produced a relatively lower impacts than that from 550 to 750 °C. The possible reasons could be that the HM salts (sulfate, carbonate, chlorate, phosphate etc.) can decompose into HM oxide or silicate at a lower temperature (≤ 550 °C). When pyrolysis temperature continues to rise (550–750 °C), Zn might be trapped and occluded into the carbon matrix of biochar as organometallic complex and crystal lattices, and the Ni oxides could further be reduced to the very stable crystal (Ni^0) (Xu et al., 2019; Li et al., 2019). The Cu is similar to Ni, the Cu-organic matter complexes in SS also can be reduced to lower valence (Cu^I) or stable crystal (Cu^0) during pyrolysis, resulting in the transformation of the Cu in F3 fraction to F4 fraction (Wang et al., 2019). More than 70.29% of Cr in biochar was F4 fraction at a higher temperature (≥ 550 °C), this might be owing to the formation of the stable compound $CaCrO_4$ (Hu et al., 2013). With respect to Pb, the species in biochars still showed very stable and mainly existed in F4 (> 97.65%) might due to the formation of stable lead phosphates in SS. The above results implied that the pyrolysis can immobilize HMs in SS by transforming the bioavailable fraction (F1 + F2) into the residual fraction (F4).

Adding OFMSW into SS affected the HMs' bioavailability in the biochar, but the level of impacts depends on the type of HMs. The most significant reductions were found in Cd where all OFMSWs, except PVC, reduced the F1 + F2 portion from 20.41% into less than 10.67% comparing to SSB-550 (Fig. 4). The similar but less significant trends were also observed for Zn and Ni. It is interesting to see that the addition of PVC tended to raise the percentages of Cu, Zn, and Cd in F1 comparing to SSB-550. This might due to the formation of chlorine-containing compounds during the pyrolytic PVC, which could activate HMs in biochar through chlorination reaction (Xia et al., 2020). The exact mechanisms of HMs immobilization associated with the OFMSW additions have not been confirmed and might require further exploration. The general mechanism should relate to the amount of organic compositions from OFMSW, which could lead to formation of different organometallic complexes for various HMs during pyrolysis.

One of important considerations is the selection of 550 °C for OFMSW mixtures. Although the higher pyrolysis temperature (750 °C) might seem to produce lowest bioavailability in the biochar, it is worth to note that a large amount of Cd can be volatilized into the bio-oil and gases which further lead to secondary pollution due to its low volatile temperature, the total HM immobilization mass is lower than 550 °C. In addition, maintaining higher pyrolysis temperature also leads to higher

energy consumption and lower biochar production, thus 550 °C can be regarded as a better optimum pyrolysis temperature. Another important note is the PVC as an OFMSW addition. Unlike many other OFMSWs that created positive synergies in the SS biochar properties, PVC demonstrated a negative effect on the bioavailable fractions (F1 + F2), which suggested that PVC must be controlled properly or even totally removed in the OFMSW-assisted pyrolysis.

3.2.3. Leaching characterization of HMs

TCLP method represents the direct availability and toxicity of HMs in SS and biochars by simulating natural leaching conditions in landfill (Nair et al., 2008; He et al., 2019), while DTPA indicates the bioavailability by displace transition HMs bound to organic matter, carbonates and metal complexes (He et al., 2019). Fig. 5 showed the leaching rates of HMs in SS and biochars and the detailed leaching contents were available in Tables S4 and S5. In TCLP (pH 2.88) extraction process (Fig. 5A), the leaching rates of Zn, Cu, Cr, Pb, Ni, and Cd in SS were 43.04%, 3.38%, 2.96%, 0.38%, 26.14%, and 12.95%, respectively. Similar high extraction rates were also observed in DTPA (Fig. 5C), suggesting that the applying SS directly into soil is not advisable as it will lead to potential threats to environment.

As to the biochar, both TCLP and DTPA extractions exhibited a continuous decline trends with the rising temperature except Cd at high temperature (Fig. 5A and C). The leaching rates of Cd in SSB-750 increase might due to the combination effects of the significant reduction of total concentration and the formation of some Cd soluble species during its volatilization at 750 °C. This again suggested that 550 °C is a better option if the major objective is to retain and immobilize the HMs in the biochar. At 550 °C, it carries high enough temperature to form the carbon matrix with more stable structures such as metal-phosphate, metal-silicate, and metal-oxide, etc. Some of the insoluble matters will be trapped in the carbon matrix or the pores of biochar (Xu et al., 2019).

Adding OFMSWs into SS further indicates the issues of PVC during the pyrolysis. Most of the results showed that PVC promotes the leaching rates in both TCLP and DTPA processes (Fig. 5B and D). This might be ascribed to the change of physiochemical property (more acidic and lower SSA value) of SSB-PVC.

3.3. Phytotoxicity and environmental risk evaluation of the SS and biochars

3.3.1. Phytotoxicity assessment

On top of the BCR and leaching tests, Fig. 6 presented the germination index (GI) and rooting length of the cucumber seeds with SS and biochars to confirm the actual impacts to the plant growth. According to the reference standard, the GI can be divided into three eco-toxicity levels: no phytotoxicity (GI > 80%), moderate phytotoxicity (50% <GI < 80%), and strong phytotoxicity (GI < 50%) (Zhang et al., 2020). The GI value of SS was 47.04% (lower than 50%, strong phytotoxicity) Fig. 6A, which was consistent with the BCR and leaching results, suggesting high bioavailability of HMs in SS. Low temperature pyrolysis at 350 °C did not change the situation but increasing the temperature from 350 °C to 550 °C, seeing remarkable improvements in GI value and the rooting length which increased from 49.06% and 11.23 mm in SSB350 to 85.66% (more than 80%) and 17.59 mm in SSB-550, respectively. Further increase the temperature from 550 to 750 °C, however, created the negative impacts, mainly attributing to a high pH of SSB-750 with strong alkaline elements inhibited the plant growth (Zhang et al., 2020). This again suggested that 550 °C is favorable for the SS detoxication via pyrolysis.

Fig. 6B showed that many OFMSWs produced the GI values higher than 80%, indicating no phytotoxicity. Bamboo sawdust (SSB-BS) leads to a slightly lower GI at 77.14%, which might due to its higher pH (9.97). PVC again exhibits a high phytotoxicity with a GI value at 27.44%, which could be attributed to the low pH and the higher HMs bioavailability of SSB-PVC.
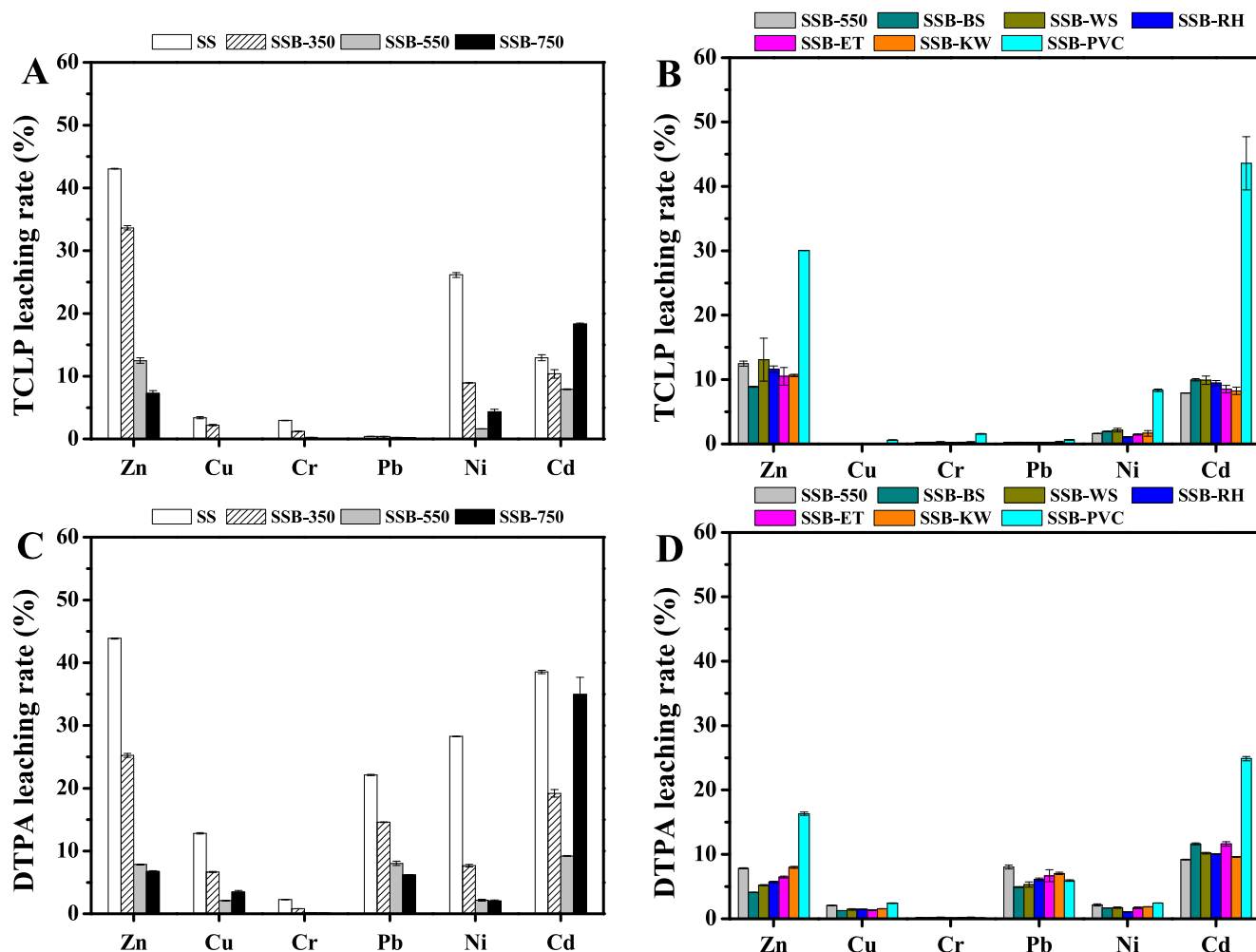
Fig. 5. Leaching rates of HMs in SS and biochars base on the TCLP extraction (A, B) and DTPA extraction (C, D). SS, sewage sludge; SSB-X, biochar derived from SS single pyrolysis at X (°C) temperature; SSB-BS, SSB-WS, SSB-RH, SSB-ET, SSB-KW, and SSB-PVC were blended biochars from co-pyrolysis SS with bamboo sawdust (BS), wood sawdust (WS), rice husk (RH), exhausted tea (ET), kitchen waste (KW), and polyvinyl chloride (PVC) at 550 °C, respectively.

Fig. 6. Germination index and root length of cucumber seeds in (A) SS and biochars derived from pyrolysis of SS alone under different temperatures, and (B) biochars from co-pyrolysis of SS and various OFMSW. SS, sewage sludge; SSB-X, biochar derived from SS single pyrolysis at X (°C) temperature; SSB-BS, SSB-WS, SSB-RH, SSB-ET, SSB-KW, and SSB-PVC were blended biochars from co-pyrolysis SS with bamboo sawdust (BS), wood sawdust (WS), rice husk (RH), exhausted tea (ET), kitchen waste (KW), and polyvinyl chloride (PVC) at 550 °C, respectively.
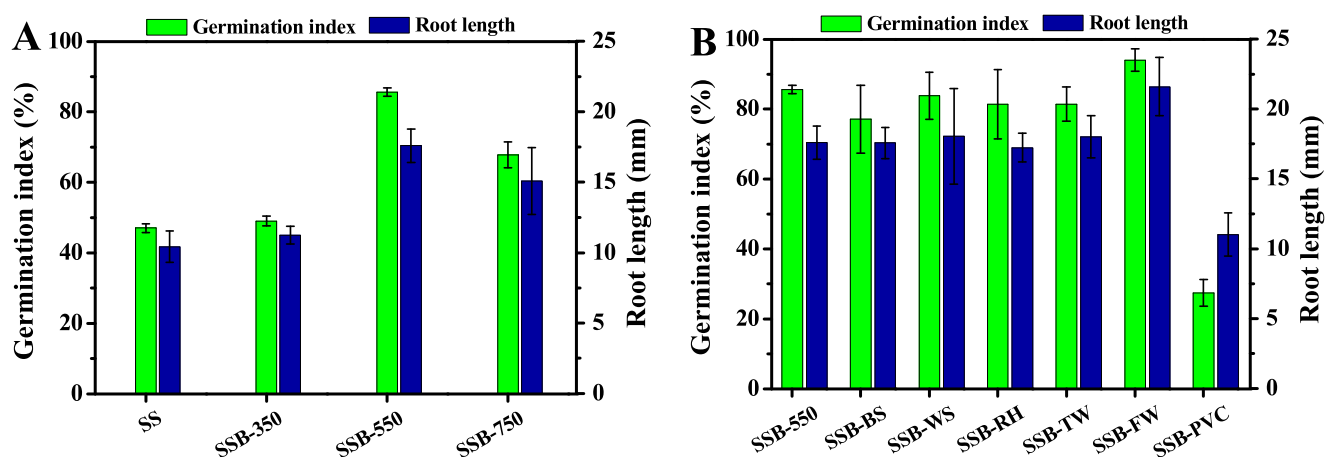
3.3.2. Environmental risk evaluation

One additional indicator of environmental risk of SS and biochars were examined using risk assessment code (RAC) and potential ecological risk index (RI). According to the values of RAC from Table 3, Zn (50.92) in SS presented a very high-risk level with RAC > 50%, and Cd (33.19) and Ni (30.83) in SS were assessed as high-risk level with

Table 3

Risk assessment codes (RAC) of HMs in SS and biochars.

Samples	Zn	Cd	Ni	Cr	Cu	Pb
SS	50.92/ VHR	33.19/ HR	30.83/ HR	4.77/ LR	1.79/ LR	0.39/ NR
SSB-350	23.53/ MR	21.76/ MR	10.49/ MR	0.98/ NR	0.46/ NR	0.14/ NR
SSB-550	20.68/ MR	11.93/ MR	8.80/LR	0.52/ NR	0.09/ NR	0.20/ NR
SSB-750	2.92/LR	1.36/LR	3.83/LR	0.38/ NR	0.08/ NR	0.18/ NR
SSB-BS	16.23/ MR	3.46/ LR	10.48/ MR	0.30/ NR	0.12/ NR	0.15/ NR
SSB-WS	16.17/ MR	3.78/ LR	7.85/LR	0.43/ NR	0.12/ NR	0.16/ NR
SSB-RH	13.17/ MR	3.95/ LR	4.87/LR	0.24/ NR	0.09/ NR	0.10/ NR
SSB-ET	14.09/ MR	2.41/ LR	9.42/LR	0.37/ NR	0.13/ NR	0.29/ NR
SSB-KW	15.67/ MR	0.96/ LR	7.59/LR	0.32/ NR	0.09/ NR	0.07/ NR
SSB-PVC	28.74/ MR	16.15/ MR	3.44/LR	0.76 /NR	1.33/ LR	0.37/ NR

SS, sewage sludge; SSB-X, biochar derived from SS single pyrolysis at X (°C) temperature; SSB-BS, SSB-WS, SSB-RH, SSB-ET, SSB-KW, and SSB-PVC were blended biochars from co-pyrolysis SS with bamboo sawdust (BS), wood sawdust (WS), rice husk (RH), exhausted tea (ET), kitchen waste (KW), and polyvinyl chloride (PVC) at 550 °C, respectively. NR, no risk (RAC ‹ 1%); LR, low risk (1%≤ RAC ‹ 10%); MR, medium risk (10%≤ RAC ‹ 30%); HR, high risk (30%≤ RAC ‹ 50%); VHR, very high risk (RAC ≥ 50%).

30%≤ RAC ‹ 50%, suggesting potentially high environmental toxicity. The data also showed that the pyrolysis helps to reduce RAC significantly and the higher temperature creates the better results. For instance, the values of RAC for Zn, Cd, and Ni decreased from 23.53, 21.76, and 10.49 in SSB-350 to 2.92, 1.36, and 3.83 in SSB-750, respectively. This indicated that the environmental risk of Zn, Cd, and Ni in SS were transformed from (very) high risk to medium risk or low risk in the biochars via pyrolysis. In addition, the values of RAC for Cr, Cu, and Pb in SS and biochars presented no-risk or low-risk levels owing to those mainly presented in F3 + F4 fractions (Fig. 3), suggesting a low toxicity to the environment. Most OFMSWs, again except PVC, had positive effects in RAC evaluation, especially for Zn and Cd. The addition of PVC, on the other hand, increased the RAC values for Zn, Cd, Cr, Cu, and Pb by 38.99%, 35.41%, 48.12%, and 1454.67%, 85.77%, respectively, comparing to that in SSB-550, indicating relative high toxicity to the environment.

Table 4 presented the RI values (potential environmental risk index for all HMs) in SS and biochars, and Table S6 showed the criteria used for risk ranking of HMs based on RI, E_r, and RI (Chen et al., 2020; Wang et al., 2019). Similar conclusions were drawn for SS that the RI values at

207.33 suggesting a high degree of HMs contamination (RI> 200, highly contaminated). Pyrolysis does decrease the RI and the rising temperature further enhance the reduction. It is worth noted that 750 °C is the only temperature that can produce the RI below the 50 threshold (34.89, low potential environmental risk). Further examine the data revealed that the significant drop for Cd (E_r = 21.99) is the main contributor. However, it should be noted that this reduction might due to the volatilization of Cd at 750 °C, indicating the overall toxicity shifting to air instead of dropping. Comparing to the SS pyrolysis alone (SSB-550), the additions of various OFMSW carried positive impacts in lowering the RI indexes. Most of the RIs dropped below 50 except SSB-RH, indicating the suitability of direct environmental application of these biochars. The RI for SSB-RH was slightly higher (55.80) might due to the higher contents of Cr and Ni in the original RH than SS.

3.4. Future perspectives and limitations

Based on our data, the additions of various OFMSW (except PVC) for co-pyrolysis with SS improved the biochar properties, reduced the total concentration and the bioavailability of HMs, and remarkably declined the potential environmental risk of the blended biochars. Given the complex synergistic reactions for co-pyrolysis process of SS and OFMSW, there are still room for improvement for future research efforts. For examples, it will be highly beneficial to explore the optimization of blended biochar properties such as pore structure, ash content, carbon content, and total concentrations of HMs, with a special focus on the operational variables including blending ratio and pyrolysis conditions, etc. In addition, the detailed mechanism of HMs immobilization during co-pyrolysis still call for further investigations. It will also be interesting to explore the fate and long-term effects of in-situ biochar applications.

4. Conclusions

This work reveals that many OFMSWs demonstrated good synergies in co-pyrolysis with SS by improving the bended biochar properties and reducing the bioavailability and toxicity of HMs in the biochar. Comparing with 350 °C and 750 °C, 550 °C is a better temperate for this process as it reached a good balance in consolidating the HMs into the biochars and preventing the Cd transforming into gaseous phases. The advantages include the improvement to more natural pH, reducing the total leaching rate of HMs, promoting the transformation from the bioavailable fractions (F1 + F2) into the residual fraction (F4), and further lowering the RI (lower than 55.80). Among the various OFMSWs, the only exception is the PVC which adversely influenced the biochar properties and environmental risk. The major reasons include its lowest pH (3.06), low SSA value (2.20 m² g⁻¹), a higher leachable rates, and the high phytotoxicity for plant growth.

In summary, this work investigated the temperature effects in the

Table 4

Ecological risk assessment of the HMs in SS, SR, and biochar.

Sample	C_f						E_r						RI
	Zn	Cu	Cr	Pb	Ni	Cd	Zn	Cu	Cr	Pb	Ni	Cd	
SS	6.53	1.67	0.60	0.01	1.81	6.01	6.53	8.37	1.20	0.06	10.86	180.31	207.33
SSB-350	2.84	1.32	0.58	0.01	1.10	3.73	2.84	6.62	1.15	0.06	6.58	111.99	129.24
SSB-550	2.93	1.16	0.42	0.02	1.09	1.51	2.93	5.80	0.85	0.11	6.52	45.25	61.47
SSB-750	1.58	1.06	0.33	0.02	0.87	0.73	1.58	5.31	0.65	0.12	5.22	21.99	34.89
SSB-BS	1.96	0.89	0.39	0.05	1.20	1.07	1.96	4.46	0.78	0.24	7.20	31.96	46.59
SSB-WS	2.07	0.75	0.41	0.03	0.97	0.71	2.07	3.77	0.82	0.17	5.83	21.41	34.06
SSB-RH	3.61	1.13	0.31	0.05	0.55	1.41	3.61	5.65	0.63	0.24	3.29	42.39	55.80
SSB-ET	1.65	0.55	0.42	0.03	1.08	0.66	1.65	2.74	0.84	0.16	6.48	19.67	31.53
SSB-KW	2.19	0.94	0.39	0.02	1.01	0.82	2.19	4.71	0.78	0.08	6.03	24.73	38.52
SSB-PVC	2.12	0.77	0.28	0.01	1.35	1.14	2.12	3.87	0.55	0.07	8.12	34.08	48.81

SS, sewage sludge; SSB-X, biochar derived from SS single pyrolysis at X (°C) temperature; SSB-BS, SSB-WS, SSB-RH, SSB-ET, SSB-KW, and SSB-PVC were blended biochars from co-pyrolysis SS with bamboo sawdust (BS), wood sawdust (WS), rice husk (RH), exhausted tea (ET), kitchen waste (KW), and polyvinyl chloride (PVC) at 550 °C, respectively.

pyrolysis process and engaged a systematic evaluation to provide further insights in selecting suitable biomass wastes from municipal solid waste as additives in SS co-pyrolysis to enhance biochar properties and immobilize the HMs in SS.

CRediT authorship contribution statement

Xingdong Wang: Methodology, Formal analysis, Investigation, Resources, Data curation, Writing-original draft, Writing-review & editing. **Victor Wei-Chung Chang:** Formal analysis, Supervision, Writing-review & editing. **Zhiwei Li:** Investigation, Resources. **Zhan Chen:** Investigation, Data curation. **Yin Wang:** Funding acquisition, Project administration, Validation, Supervision, Writing-review & editing.

Declaration of Competing Interest

The authors declare that they have no known competing financial interests or personal relationships that could have appeared to influence the work reported in this paper.

Acknowledgments

Appendix A. Supporting information

Supplementary data associated with this article can be found in the online version at doi:10.1016/j.jhazmat.2021.125200.

References

Agrafioti, E., Bouras, G., Kalderis, D., Diamadopoulos, E., 2013. Biochar production by sewage sludge pyrolysis. J. Anal. Appl. Pyrolysis 101, 72–78. https://doi.org/10.1016/j.jaap.2013.02.010.

Ahmed, M.J., Hameed, B.H., 2020. Insight into the co-pyrolysis of different blended feedstocks to biochar for the adsorption of organic and inorganic pollutants: a review. J. Clean. Prod. 265, 121762 https://doi.org/10.1016/j.jclepro.2020.121762.

Cao, B., Sun, Y., Guo, J., Wang, S., Yuan, J., Esakkimuthu, S., Bernard Uzoejinwa, B., Yuan, C., Abomohra, A.E.-F., Qian, L., Liu, L., Li, B., He, Z., Wang, Q., 2019. Synergistic effects of co-pyrolysis of macroalgae and polyvinyl chloride on bio-oil/bio-char properties and transferring regularity of chlorine. Fuel 246, 319–329. https://doi.org/10.1016/j.fuel.2019.02.037.

Chanaka Udayanga, W.D., Veksha, A., Giannis, A., Lisak, G., Chang, V.W.C., Lim, T.-T., 2018. Fate and distribution of heavy metals during thermal processing of sewage sludge. Fuel 226, 721–744. https://doi.org/10.1016/j.fuel.2018.04.045.

Chanaka Udayanga, W.D., Veksha, A., Giannis, A., Liang, Y.N., Lisak, G., Hu, X., Lim, T. T., 2019. Insights into the speciation of heavy metals during pyrolysis of industrial sludge. Sci. Total Environ. 691, 232–242. https://doi.org/10.1016/j.scitotenv.2019.07.095.

Chen, J., Tang, S., Yan, F., Zhang, Z., 2020. Efficient recovery of phosphorus in sewage sludge through hydroxylapatite enhancement formation aided by calcium-based additives. Water Res. 171, 115450 https://doi.org/10.1016/j.watres.2019.115450.

Chen, L., Liao, Y., Ma, X., Niu, Y., 2020. Effect of co-combusted sludge in waste incinerator on heavy metals chemical speciation and environmental risk of horizontal flue ash. Waste Manag. 102, 645–654. https://doi.org/10.1016/j.wasman.2019.11.027.

Chen, Q., Liu, H., Ko, J., Wu, H., Xu, Q., 2019. Structure characteristics of bio-char generated from co-pyrolysis of wooden waste and wet municipal sewage sludge. Fuel Process. Technol. 183, 48–54. https://doi.org/10.1016/j.fuproc.2018.11.005.

Chen, Z., Yu, G., Wang, Y., Liu, X., Wang, X., 2019. Research on synergistically hydrothermal treatment of municipal solid waste incineration fly ash and sewage sludge. Waste Manag. 100, 182–190. https://doi.org/10.1016/j.wasman.2019.09.006.

Chhabra, V., Bhattacharya, S., Shastri, Y., 2019. Pyrolysis of mixed municipal solid waste: characterisation, interaction effect and kinetic modelling using the thermogravimetric approach. Waste Manag. 90, 152–167. https://doi.org/10.1016/j.wasman.2019.03.048.

Devi, P., Saroha, A.K., 2014. Risk analysis of pyrolyzed biochar made from paper mill effluent treatment plant sludge for bioavailability and eco-toxicity of heavy metals. Bioresour. Technol. 162, 308–315. https://doi.org/10.1016/j.biortech.2014.03.093.

Dong, Q., Zhang, S., Wu, B., Pi, M., Xiong, Y., Zhang, H., 2019. Co-pyrolysis of sewage sludge and rice straw: thermal behavior and char characteristic evaluations. Energy Fuels 34, 607–615. https://doi.org/10.1021/acs.energyfuels.9b03800.

Dou, X., Chen, D., Hu, Y., Feng, Y., Dai, X., 2017. Carbonization of heavy metal impregnated sewage sludge oriented towards potential co-disposal. J. Hazard. Mater. 321, 132–145. https://doi.org/10.1016/j.jhazmat.2016.09.010.

Du, J., Zhang, L., Liu, T., Xiao, R., Li, R., Guo, D., Qiu, L., Yang, X., Zhang, Z., 2019. Thermal conversion of a promising phytoremediation plant (Symphytum officinale L.) into biochar: dynamic of potentially toxic elements and environmental acceptability assessment of the biochar. Bioresour. Technol. 274, 73–82. https://doi.org/10.1016/j.biortech.2018.11.077.

El-Naggar, A., Lee, S.S., Rinklebe, J., Farooq, M., Song, H., Sarmah, A.K., Zimmerman, A. R., Ahmad, M., Shaheen, S.M., Ok, Y.S., 2019. Biochar application to low fertility soils: a review of current status, and future prospects. Geoderma 337, 536–554. https://doi.org/10.1016/j.geoderma.2018.09.034.

Fan, J., Li, Y., Yu, H., Li, Y., Yuan, Q., Xiao, H., Li, F., Pan, B., 2020. Using sewage sludge with high ash content for biochar production and Cu(II) sorption. Sci. Total Environ. 713, 136663 https://doi.org/10.1016/j.scitotenv.2020.136663.

Hagemann, N., Joseph, S., Schmidt, H.P., Kammann, C.I., Harter, J., Borch, T., Young, R. B., Varga, K., Taherymoosavi, S., Elliott, K.W., McKenna, A., Albu, M., Mayrhofer, C., Obst, M., Conte, P., Dieguez-Alonso, A., Orsetti, S., Subdiaga, E., Behrens, S., Kappler, A., 2017. Organic coating on biochar explains its nutrient retention and stimulation of soil fertility. Nat. Commun. 8, 1089. https://doi.org/10.1038/s41467-017-01123-0.

Han, J., Wang, X., Yue, J., Gao, S., Xu, G., 2014. Catalytic upgrading of coal pyrolysis tar over char-based catalysts. Fuel Process. Technol. 122, 98–106. https://doi.org/10.1016/j.fuproc.2014.01.033.

He, J., Strezov, V., Kan, T., Weldekidan, H., Asumadu-Sarkodie, S., Kumar, R., 2019. Effect of temperature on heavy metal(loid) deportment during pyrolysis of Avicennia marina biomass obtained from phytoremediation. Bioresour. Technol. 278, 214–222. https://doi.org/10.1016/j.biortech.2019.01.101.

Ho, S.H., Chen, Y.D., Yang, Z.K., Nagarajan, D., Chang, J.S., Ren, N.Q., 2017. High-efficiency removal of lead from wastewater by biochar derived from anaerobic digestion sludge. Bioresour. Technol. 246, 142–149. https://doi.org/10.1016/j.biortech.2017.08.025.

Hu, H.Y., Liu, H., Shen, W.Q., Luo, G.Q., Li, A.J., Lu, Z.L., Yao, H., 2013. Comparison of CaO's effect on the fate of heavy metals during thermal treatment of two typical types of MSWI fly ashes in China. Chemosphere 93, 590–596. https://doi.org/10.1016/j.chemosphere.2013.05.077.

Huang, H.-J., Yang, T., Lai, F.-Y., Wu, G.-Q., 2017. Co-pyrolysis of sewage sludge and sawdust/rice straw for the production of biochar. J. Anal. Appl. Pyrolysis 125, 61–68. https://doi.org/10.1016/j.jaap.2017.04.018.

Huang, H.J., Yuan, X.Z., 2016. The migration and transformation behaviors of heavy metals during the hydrothermal treatment of sewage sludge. Bioresour. Technol. 200, 991–998. https://doi.org/10.1016/j.biortech.2015.10.099.

Jin, J., Li, Y., Zhang, J., Wu, S., Cao, Y., Liang, P., Zhang, J., Wong, M.H., Wang, M., Shan, S., Christie, P., 2016. Influence of pyrolysis temperature on properties and environmental safety of heavy metals in biochars derived from municipal sewage sludge. J. Hazard Mater. 320, 417–426. https://doi.org/10.1016/j.jhazmat.2016.08.050.

Jin, J., Wang, M., Cao, Y., Wu, S., Liang, P., Li, Y., Zhang, J., Zhang, J., Wong, M.H., Shan, S., Christie, P., 2017. Cumulative effects of bamboo sawdust addition on pyrolysis of sewage sludge: biochar properties and environmental risk from metals. Bioresour. Technol. 228, 218–226. https://doi.org/10.1016/j.biortech.2016.12.103.

Kistler, R.C., Widmer, F., Brunner, P.H., 1987. Behavior of chromium, nickel, copper, zinc, cadmium, mercury, and lead during the pyrolysis of sewage sludge. Environ. Sci. Technol. 21, 704–708. https://doi.org/10.1021/es00161a012.

Li, C., Wang, X., Zhang, G., Li, J., Li, Z., Yu, G., Wang, Y., 2018. A process combining hydrothermal pretreatment, anaerobic digestion and pyrolysis for sewage sludge dewatering and co-production of biogas and biochar: pilot-scale verification. Bioresour. Technol. 254, 187–193. https://doi.org/10.1016/j.biortech.2018.01.045.

Li, R., Huang, H., Wang, J.J., Liang, W., Gao, P., Zhang, Z., Xiao, R., Zhou, B., Zhang, X., 2019. Conversion of Cu(II)-polluted biomass into an environmentally benign Cu nanoparticles-embedded biochar composite and its potential use on cyanobacteria inhibition. J. Clean. Prod. 216, 25–32. https://doi.org/10.1016/j.jclepro.2019.01.186.

Li, Z., Ma, Z., van der Kuijp, T.J., Yuan, Z., Huang, L., 2014. A review of soil heavy metal pollution from mines in China: pollution and health risk assessment. Sci. Total Environ. 468–469, 843–853. https://doi.org/10.1016/j.scitotenv.2013.08.090.

Li, Z., Deng, H., Yang, L., Zhang, G., Li, Y., Ren, Y., 2018. Influence of potassium hydroxide activation on characteristics and environmental risk of heavy metals in chars derived from municipal sewage sludge. Bioresour. Technol. 256, 216–223. https://doi.org/10.1016/j.biortech.2018.02.013.

Liu, W.J., Li, W.W., Jiang, H., Yu, H.Q., 2017. Fates of chemical elements in biomass during its pyrolysis. Chem. Rev. 117, 6367–6398. https://doi.org/10.1021/acs.chemrev.6b00647.

Liu, Y., Ran, C., Siddiqui, A.R., Siyal, A.A., Song, Y., Dai, J., Chtaeva, P., Fu, J., Ao, W., Deng, Z., Jiang, Z., Zhang, T., 2020. Characterization and analysis of sludge char prepared from bench-scale fluidized bed pyrolysis of sewage sludge. Energy 200, 117398. https://doi.org/10.1016/j.energy.2020.117398.

Lu, P., Huang, Q., Bourtsalas, A.C., Chi, Y., Yan, J., 2018. Synergistic effects on char and oil produced by the co-pyrolysis of pine wood, polyethylene and polyvinyl chloride. Fuel 230, 359–367. https://doi.org/10.1016/j.fuel.2018.05.072.

Marin-Batista, J.D., Mohedano, A.F., Rodríguez, J.J., de la Rubia, M.A., 2020. Energy and phosphorous recovery through hydrothermal carbonization of digested sewage

sludge. Waste Manag. 105, 566–574. https://doi.org/10.1016/j.wasman.2020.03.004.

Nair, A., Juwarkar, A.A., Devotta, S., 2008. Study of speciation of metals in an industrial sludge and evaluation of metal chelators for their removal. J. Hazard. Mater. 152, 545–553. https://doi.org/10.1016/j.jhazmat.2007.07.054.

Nottingham, A.T., Meir, P., Velasquez, E., Turner, B.L., 2020. Soil carbon loss by experimental warming in a tropical forest. Nature 584, 234–237. https://doi.org/10.1038/s41586-020-2566-4.

Palansooriya, K.N., Shaheen, S.M., Chen, S.S., Tsang, D.C.W., Hashimoto, Y., Hou, D., Bolan, N.S., Rinklebe, J., Ok, Y.S., 2020. Soil amendments for immobilization of potentially toxic elements in contaminated soils: a critical review. Environ. Int. 134, 105046 https://doi.org/10.1016/j.envint.2019.105046.

Shen, X., Zeng, J., Zhang, D., Wang, F., Li, Y., Yi, W., 2020. Effect of pyrolysis temperature on characteristics, chemical speciation and environmental risk of Cr, Mn, Cu, and Zn in biochars derived from pig manure. Sci. Total Environ. 704, 135283 https://doi.org/10.1016/j.scitotenv.2019.135283.

Shi, W., Liu, C., Ding, D., Lei, Z., Yang, Y., Feng, C., Zhang, Z., 2013. Immobilization of heavy metals in sewage sludge by using subcritical water technology. Bioresour. Technol. 137, 18–24. https://doi.org/10.1016/j.biortech.2013.03.106.

Soomro, A.F., Abbasi, I.A., Ni, Z., Ying, L., Liu, J., 2020. Influence of temperature on enhancement of volatile fatty acids fermentation from organic fraction of municipal solid waste: synergism between food and paper components. Bioresour. Technol. 304, 122980 https://doi.org/10.1016/j.biortech.2020.122980.

Sun, S., Huang, X., Lin, J., Ma, R., Fang, L., Zhang, P., Qu, J., Zhang, X., Liu, Y., 2018. Study on the effects of catalysts on the immobilization efficiency and mechanism of heavy metals during the microwave pyrolysis of sludge. Waste Manag. 77, 131–139. https://doi.org/10.1016/j.wasman.2018.04.046.

Sun, Y., Chen, G., Yan, B., Cheng, Z., Ma, W., 2020. Behaviour of mercury during Co-incineration of sewage sludge and municipal solid waste. J. Clean. Prod. 253, 119969 https://doi.org/10.1016/j.jclepro.2020.119969.

Tang, Y., Huang, Q., Sun, K., Chi, Y., Yan, J., 2018. Co-pyrolysis characteristics and kinetic analysis of organic food waste and plastic. Bioresour. Technol. 249, 16–23. https://doi.org/10.1016/j.biortech.2017.09.210.

Tian, Y., Li, J., Yan, X., Whitcombe, T., Thring, R., 2019. Co-pyrolysis of metal contaminated oily waste for oil recovery and heavy metal immobilization. J. Hazard. Mater. 373, 1–10. https://doi.org/10.1016/j.jhazmat.2019.03.061.

Tokmurzin, D., Kuspangaliyeva, B., Aimbetov, B., Abylkhani, B., Inglezakis, V., Anthony, E.J., Sarbassov, Y., 2020. Characterization of solid char produced from pyrolysis of the organic fraction of municipal solid waste, high volatile coal and their blends. Energy 191, 116562. https://doi.org/10.1016/j.energy.2019.116562.

Wang, X., Li, C., Zhang, B., Lin, J., Chi, Q., Wang, Y., 2016. Migration and risk assessment of heavy metals in sewage sludge during hydrothermal treatment combined with pyrolysis. Bioresour. Technol. 221, 560–567. https://doi.org/10.1016/j.biortech.2016.09.069.

Wang, X., Chi, Q., Liu, X., Wang, Y., 2019. Influence of pyrolysis temperature on characteristics and environmental risk of heavy metals in pyrolyzed biochar made from hydrothermally treated sewage sludge. Chemosphere 216, 698–706. https://doi.org/10.1016/j.chemosphere.2018.10.189.

Wang, X., Li, C., Li, Z., Yu, G., Wang, Y., 2019. Effect of pyrolysis temperature on characteristics, chemical speciation and risk evaluation of heavy metals in biochar derived from textile dyeing sludge. Ecotoxicol. Environ. Saf. 168, 45–52. https://doi.org/10.1016/j.ecoenv.2018.10.022.

Wang, Z., Xie, L., Liu, K., Wang, J., Zhu, H., Song, Q., Shu, X., 2019. Co-pyrolysis of sewage sludge and cotton stalks. Waste Manag. 89, 430–438. https://doi.org/10.1016/j.wasman.2019.04.033.

Wang, Z., Liu, K., Xie, L., Zhu, H., Ji, S., Shu, X., 2019. Effects of residence time on characteristics of biochars prepared via co-pyrolysis of sewage sludge and cotton stalks. J. Anal. Appl. Pyrolysis 142, 104659. https://doi.org/10.1016/j.jaap.2019.104659.

Wong, J., Li, K., Fang, M., Su, D., 2001. Toxicity evaluation of sewage sludges in Hong Kong. Environ. Int. 27, 373–380. https://doi.org/10.1016/S0160-4120(01)00088-5.

Xia, Y., Tang, Y., Shih, K., Li, B., 2020. Enhanced phosphorus availability and heavy metal removal by chlorination during sewage sludge pyrolysis. J. Hazard. Mater. 382, 121110 https://doi.org/10.1016/j.jhazmat.2019.121110.

Xu, J., Liu, C., Hsu, P.C., Zhao, J., Wu, T., Tang, J., Liu, K., Cui, Y., 2019. Remediation of heavy metal contaminated soil by asymmetrical alternating current electrochemistry. Nat. Commun. 10, 2440. https://doi.org/10.1038/s41467-019-10472-x.

Xu, Y., Qi, F., Bai, T., Yan, Y., Wu, C., An, Z., Luo, S., Huang, Z., Xie, P., 2019. A further inquiry into co-pyrolysis of straws with manures for heavy metal immobilization in manure-derived biochars. J. Hazard. Mater. 380, 120870 https://doi.org/10.1016/j.jhazmat.2019.120870.

Yang, Y., Heaven, S., Venetsaneas, N., Banks, C.J., Bridgwater, A.V., 2018. Slow pyrolysis of organic fraction of municipal solid waste (OFMSW): Characterisation of products and screening of the aqueous liquid product for anaerobic digestion. Appl. Energy 213, 158–168. https://doi.org/10.1016/j.apenergy.2018.01.018.

Yin, G., Song, X., Tao, L., Sarkar, B., Sarmah, A.K., Zhang, W., Lin, Q., Xiao, R., Liu, Q., Wang, H., 2020. Novel Fe-Mn binary oxide-biochar as an adsorbent for removing Cd (II) from aqueous solutions. Chem. Eng. J. 389, 124465 https://doi.org/10.1016/j.cej.2020.124465.

Yuan, H., Lu, T., Huang, H., Zhao, D., Kobayashi, N., Chen, Y., 2015. Influence of pyrolysis temperature on physical and chemical properties of biochar made from sewage sludge. J. Anal. Appl. Pyrolysis 112, 284–289. https://doi.org/10.1016/j.jaap.2015.01.010.

Yuan, X., Huang, H., Zeng, G., Li, H., Wang, J., Zhou, C., Zhu, H., Pei, X., Liu, Z., Liu, Z., 2011. Total concentrations and chemical speciation of heavy metals in liquefaction residues of sewage sludge. Bioresour. Technol. 102, 4104–4110. https://doi.org/10.1016/j.biortech.2010.12.055.

Zhang, P., Zhang, X., Li, Y., Han, L., 2020. Influence of pyrolysis temperature on chemical speciation, leaching ability, and environmental risk of heavy metals in biochar derived from cow manure. Bioresour. Technol. 302, 122850 https://doi.org/10.1016/j.biortech.2020.122850.

Zhang, T., Wang, Y., Liu, X., Lü, J., Li, J., 2019. Functions of phosphorus additives on immobilizing heavy metal cadmium in the char through pyrolysis of contaminated biomass. J. Anal. Appl. Pyrolysis 144, 104721. https://doi.org/10.1016/j.jaap.2019.104721.

Zheng, C., Ma, X., Yao, Z., Chen, X., 2019. The properties and combustion behaviors of hydrochars derived from co-hydrothermal carbonization of sewage sludge and food waste. Bioresour. Technol. 285, 121347 https://doi.org/10.1016/j.biortech.2019.121347.

Zielinska, A., Oleszczuk, P., 2016. Effect of pyrolysis temperatures on freely dissolved polycyclic aromatic hydrocarbon (PAH) concentrations in sewage sludge-derived biochars. Chemosphere 153, 68–74. https://doi.org/10.1016/j.chemosphere.2016.02.118.